Available online at www.sciencedirect.com
ScienceDirect
Nuclear Instruments and Methods in Physics Research A 567 (2006) 78–82
NUCLEAR INSTRUMENTS & METHODS IN PHYSICS RESEARCH Section A
www.elsevier.com/locate/nima

Large area silicon photomultipliers: Performance and applications

P. Buzhan[a], B. Dolgoshein[a,*], L. Filatov[b], A. Ilyin[a], V. Kaplin[a], A. Karakash[a], S. Klemin[b], R. Mirzoyan[c], A.N. Otte[c], E. Popova[a], V. Sosnovtsev[a], M. Teshima[c]

[a]*Moscow Engineering and Physics Institute, Kashirskoe Shosse 31, 115409 Moscow, Russia*
[b]*"Pulsar" Enterprise, Okruzhnoj Proezd 27, Moscow, Russia*
[c]*Max-Plank Institute for Physics, Fohringer Ring 6, 80805 Munich, Germany*

Available online 9 June 2006

Abstract

The Silicon Photomultipliers (SiPMs) with large area up to $10 \times 10\,mm^2$ are considered and their optimal parameters, such as efficiency, gain, dark rate, afterpulsing probability and optical crosstalk are discussed. The $3 \times 3\,mm^2$ SiPM is described and its performance is demonstrated. Three examples of $3 \times 3\,mm^2$ SiPM application are given: (1) transition radiation X-ray detection; (2) time of flight measurements with fast scintillators; (3) detection of PET gammas using LYSO crystals. Corresponding experimental results are presented and discussed.

PACS: 29.40.Mc; 85.60.Gz; 87.58.Fg

Keywords: Silicon photomultiplier; Transition radiation detection; Time-of-flight measurements; PET gammas detection

1. Three steps in silicon Geiger-mode avalanche detectors development

1.1. First step

The single photon counters, based on single pixel Geiger-mode silicon avalanche diode (Single Photon Avalanche Diodes—SPADs) were a subject of intensive developments since 1960s [1] (see also review paper [2]). SPAD is actually a single photon counter with a size of $20-200\,\mu m$, working in Geiger-mode at operational bias voltage of 10–20% higher then the breakdown voltage, where the Geiger discharge is quenched by passive quenching (external resistor) or actively (by special quenching circuit).

1.2. Second step: from SPAD to SiPM

The Silicon Photomultiplier (SiPM) is multipixel (multi-SPAD) silicon photodiode with a number up to a few thousand independent micropixels (with typical size of $20-30\,\mu m$) joined together on common substrate and working on common load [3,4]. Each pixel detects the photoelectrons with a gain of about 10^6. The SiPM is already an analogue device with area of typically $1 \times 1\,mm^2$ which can measure the light intensity (number of photoelectrons).

1.3. Next step: large area (up to $10 \times 10\,mm^2$) SiPMs

Large area is required for a number of new SiPM applications, such as particle and astroparticle physics, positron emission tomography (PET) and others.

This paper describes the optimal parameters of large area SiPMs, first experience of design, production and performance of $3 \times 3\,mm^2$ area SiPM and three experimental examples of new applications of such large area SiPM.

2. Optimal parameters and limitations for a large area SiPM

The main goal for any multipixel SiPM is a high Photon Detection Efficiency (PDE). $PDE = QE(\lambda) \times$ packing

*Corresponding author. Tel./fax: +007 095 3247105.
E-mail address: boris@mail.cern.ch (B. Dolgoshein).

0168-9002/$ - see front matter © 2006 Elsevier B.V. All rights reserved.
doi:10.1016/j.nima.2006.05.072

efficiency × Geiger efficiency, where QE(λ) is quantum efficiency for given wavelength, packing (geometrical) efficiency = (sensitive area)/(total area), Geiger efficiency is probability for photoelectron to fire a pixel, which depends on overvoltage $V - V_{\text{breakdown}}$. The packing efficiency is larger for large pixel size (or pixel capacitance C_{pix}), that means the higher SiPM Gain = $C_{\text{pix}} \times (V - V_{\text{bd}})$. However, there are at least four reasons limiting the gain.

2.1. First reason of gain limitation: SiPM dark rate (DR)

The typical value of a single pixel DR is ~1 MHz/mm^2 (at room temperature), see Fig. 1. This means that for 10 × 10 mm^2 SiPM, the DR is expected at the level of 100 MHz (at room temperature) or even higher, taking into account the DR increase with overvoltage ($V - V_{\text{bd}}$) due to electric field-assisted tunneling effect (see Fig. 1). Therefore, a deep cooling of the large area SiPM does not help much and moderate cooling (−30 to − 50 °C) can give a reasonable DR reduction by factor of ~100, limiting the practical SiPM area at the level of 100 mm^2.

2.2. Second reason of gain limitation: the power dissipation

Very high DR leads to high-power dissipation in large area SiPM. The estimates show that for a gain (2−5) × 10^7 and 100 mm^2 area of SiPM, the mean power dissipation is of the order of 10 mW. With a thermal resistance from SiPM junctions to the heat sink of ~1 °C/mW [2] this may increase the junction temperature by ~10 °C and decrease the gain by factor 1.5–2.0. This also limits the high-gain SiPM area at the level of ~100 mm^2 for moderate cooling (−30 to − 50 °C). These two first reasons limit the area of high-gain, high-overvoltage (that is high PDE) SiPMs, working at room temperature, at the level of ~10 mm^2 (3 × 3 mm^2).

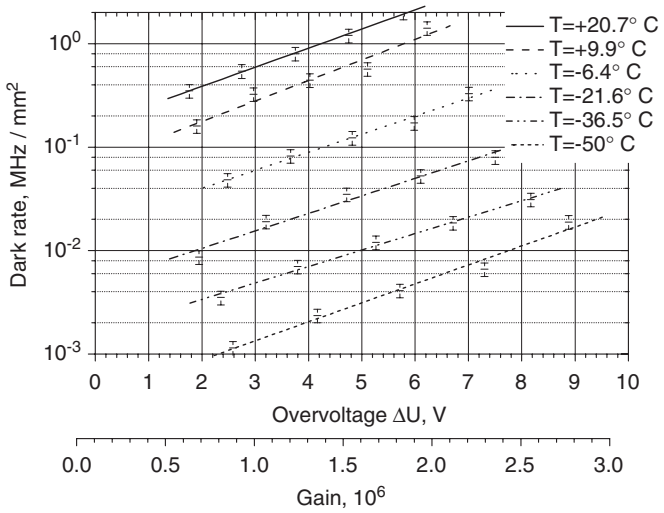

Fig. 1. Dark rate of 1 × 1 mm^2 SiPM vs gain (overvoltage).

2.3. Third reason of gain limitation: afterpulsing (AP)

AP (trapping of the electrons during discharge and their delayed release) can increase considerably the DR. Fig. 2 shows the AP, measured for 1 × 1 mm^2 SiPM with a gain of 1.3 × 10^6 (at room temperature). As expected [5] AP is high for small delay and can increase the DR by factor of ~2 for high-gain SiPM (~(2−5) × 10^7). Therefore, the single pixel recovery time of order of 1 μs is needed for suppression of AP. The cooling does not help because it increases the traps lifetime [5].

2.4. Fourth reason of gain limitation: optical crosstalk (OC)

OC is originated from secondary light emitted in Geiger discharge (~10^{-5} photons/one electron [5]). The OC violates the pixel independence and Poisson statistics of fired pixels, that is Excess Noise Factor (ENF) becomes too large for high gain (because a number of secondary photons is proportional to gain). Fig. 3 shows the experimental measurements of OC versus gain. OC is determinated as a probability that a 20 × 20 μm^2 pixel is fired by secondary photons, created in neighboring pixel, positioned at distances from 32 to 128 μm. One can see that OC increases drastically with the gain. From Fig. 3 data, we can estimate the effective absorption length l_{ab} in Si and wavelength of secondary photons: $l_{\text{ab}}(\text{Si}) \approx 50\,\mu\text{m}$, $\lambda \approx 1000$ nm. To conclude, in order to achieve high gain (high PDE) we need to suppress the OC significantly. For this purpose we have produced a special test structure of the SiPM 1 × 1 mm^2 with OC suppression. One can see the effect of OC suppression in Fig. 4a, b. Fig. 4a shows pulse height distribution (dark noise, $n_{\text{phe}} \approx 0.1$ within gate of 80 ns) for reference SiPM structure with standard topology. Pulse height distribution in Fig. 4a demonstrates high-level OC for gain of 3 × 10^6. Pulse height distribution in Fig. 4b for structure with OC suppression is compatible with Poisson statistics even for the gain ≈ 3 × 10^7.

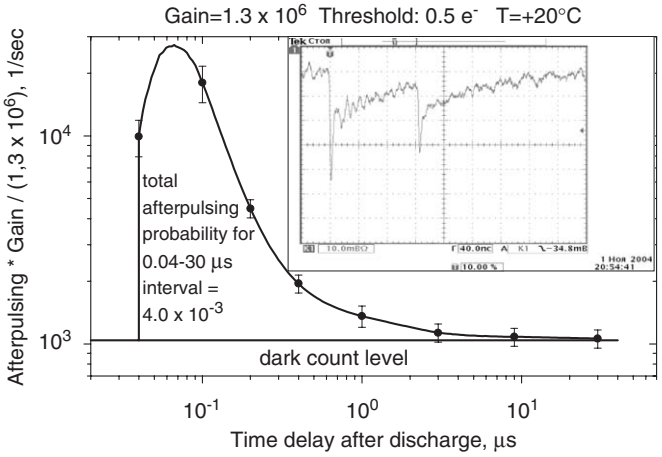

Fig. 2. Afterpulsing probability for 1 × 1 mm^2 SiPM vs time delay.

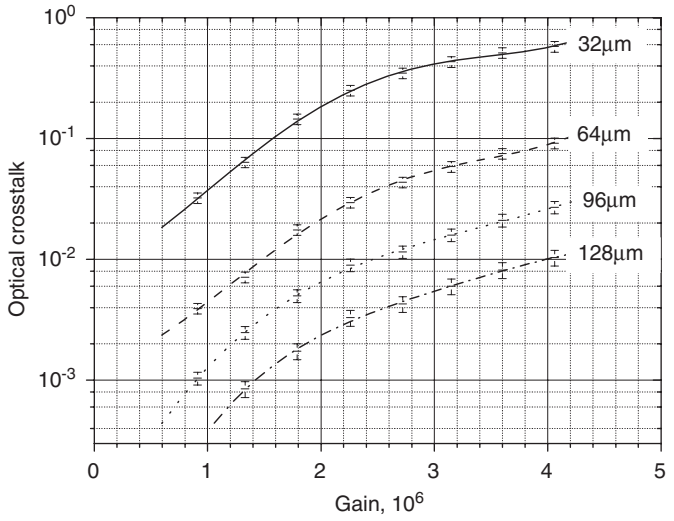

Fig. 3. Optical crosstalk vs gain between two pixels located at the distance 32–128 μm from each other.

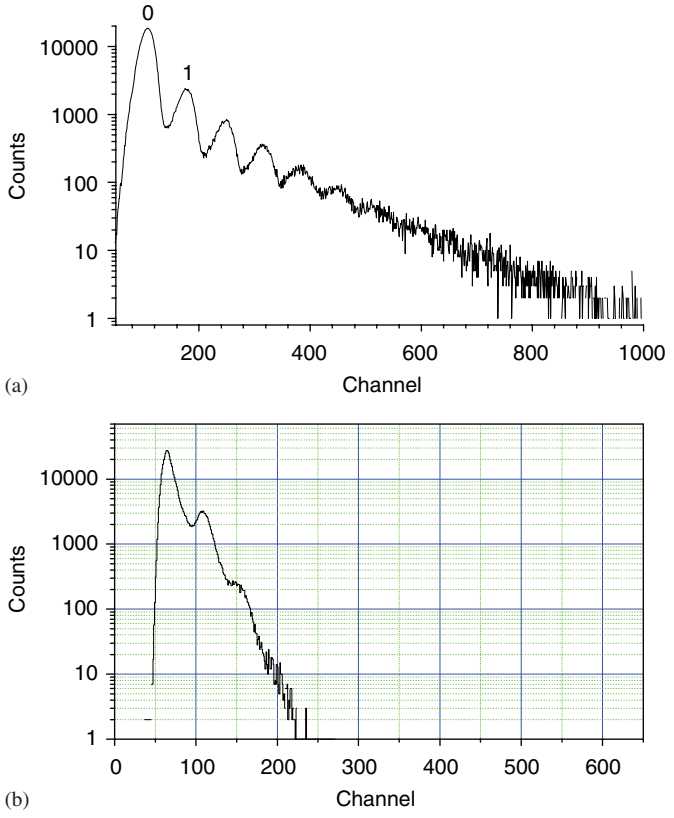

Fig. 4. (a,b) Optical crosstalk (OC) for $1 \times 1\,mm^2$ SiPM, measured as the pulse height distribution: no OC suppression (a); with OC suppression (b, preliminary data).

Following previous considerations we can formulate the optimal large area (up to $100\,mm^2$) SiPM parameters to achieve the high PDE at the level of 40–50%:

- packing efficiency $\approx 80\%$ (pixel $100 \times 100\,\mu m^2$);
- gain $(2-5) \times 10^7$;
- DR: for single photon detection $<10\,kHz/mm^2$ (cooling -30 to $-50\,^{\circ}C$) for detection of $\geqslant 10-20$ photoelectrons $\sim 1\,MHz/mm^2$ (room temperature);
- AP probability: suppression down to $<10\%$ (pixel recovery time $\sim 1\,\mu s$);
- OC: suppression down to few % (special SiPM topology).

3. $3 \times 3\,mm^2$ SiPM, properties and performance

Fig. 5 shows the microphoto of a $3 \times 3\,mm^2$ SiPM. Its main parameters are:

- sensitive area $3 \times 3\,mm^2$, number of pixels 5625;
- depletion region: $\sim 1\,\mu m$, pixel size: $30 \times 30\,\mu m^2$;
- working voltage: 20–28 V, gain: $(1-2) \times 10^6$;
- packing efficiency: $\sim 60\%$;
- Geiger efficiency: $\sim 50\%$;
- DR (room temperature): $\sim 20\,MHz$;
- single pixel recovery time: $1\,\mu s$;
- OC: 30–50%.

PDE vs wavelength for $3 \times 3\,mm^2$ SiPM is shown in Fig. 6.

4. Three examples of $3 \times 3\,mm^2$ SiPM applications

4.1. Transition radiation X-ray detectors

Transition radiation X-ray detectors are based on very thin heavy scintillators. The heavy crystal + SiPM approach looks promising and robust, especially for space physics applications. Multiset TR detectors is feasible because of the compactness and the low mass ($<1\%\ X_0$) of SiPM. The small test prototype, containing $3 \times 3\,mm^2$ SiPM + $70\,\mu m$ YAP:Ce crystal has been exposed on DESY electron test beam with energy of 3 GeV. In order to match the YAP:Ce crystal light signal (wavelength of 380 nm) with a SiPM maximal PDE (see Fig. 6) we used

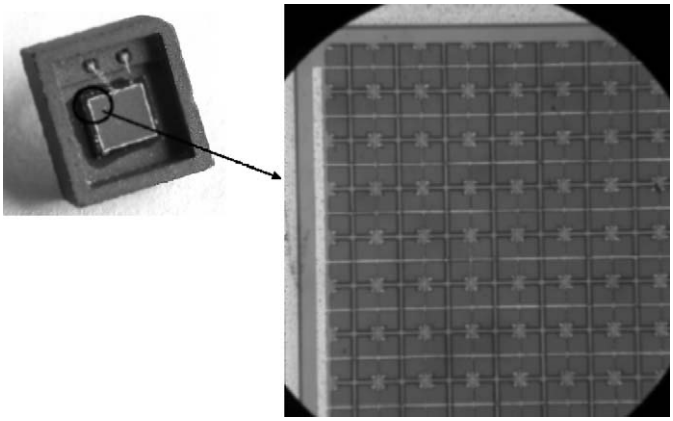

Fig. 5. SiPM $3 \times 3\,mm^2$, 5625 pixels.

WLS layer (BBQ). The results of such a detection of TR X-rays produced in TR radiator (1550 polypropylene foils) are shown in Fig. 7. One can conclude that SiPM + heavy crystal system is quite promising as a base element even for large-scale TR detectors, provided large area ($10 \times 10\,mm^2$) SiPM with high PDE and low OC will be available.

4.2. Time-of-flight measurements

We can use large area SiPMs for time-of-flight (TOF) measurements in high-energy physics (see Ref. [6]). The SiPM is intrinsically a very fast device with a single photoelectron timing resolution at 100 ps FWHM [7]). TOF system studied consisted of fast PMT FEU 187 + Cherenkov radiator (timing resolution $\sigma = 48.5$ ps) and SiPM $3 \times 3\,mm^2$ + plastic scintillator BC418 ($3 \times 3 \times 40\,mm^3$, decay time 1.4 ns). The particle beam (3 GeV electrons test beam DESY) crossed plastic scintillator along the larger size and gave a SiPM signal of about 100 mV without any amplification. The electronics (constant fraction discriminator + TDC) has an internal timing resolution of 31.5 ps. Fig. 8 shows the test beam TOF results with a total timing resolution of 66 ps. After subtraction of the timing resolution of PMT and electronics, one can obtain the SiPM + BC418 system resolution: $\sigma(\text{SiPM} + \text{BC418}) = 32$ ps. Such a result confirms the high-potential TOF system based on large area SiPM + fast plastic scintillator elements.

4.3. Positron emission tomography (PET)

The possibility of SiPM usage for PET has been demonstrated in Ref. [8] for small area ($1 \times 1\,mm^2$) SiPM. Area of SiPM ($3 \times 3\,mm^2$) is matched better with typical size of heavy crystals (LSO, LYSO) used for PET, allowing to have more light collected and to improve the pulse height and timing resolution of the PET tomograph. Fig. 9 shows the pulse height distribution obtained by system SiPM $3 \times 3\,mm^2$ + LYSO crystal $3 \times 3 \times 20\,mm^3$ for positron annihilation gammas of 511 keV. A pulse height resolution of 17.5% (FWHM) has been measured. Fast

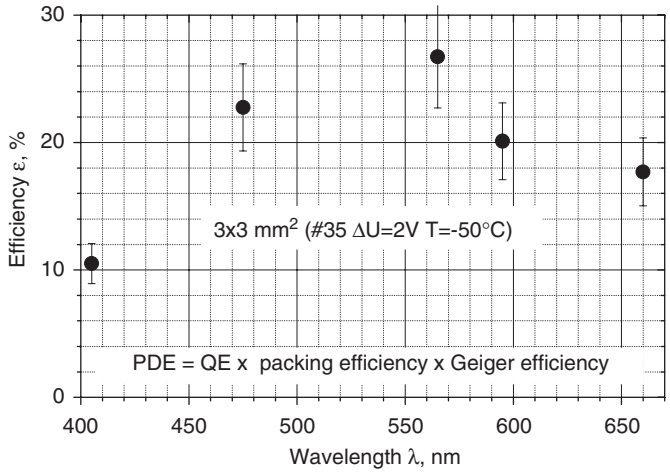

Fig. 6. Photon Detection Efficiency vs wavelength for $3 \times 3\,mm^2$ SiPM, $T = -50\,^{\circ}C$.

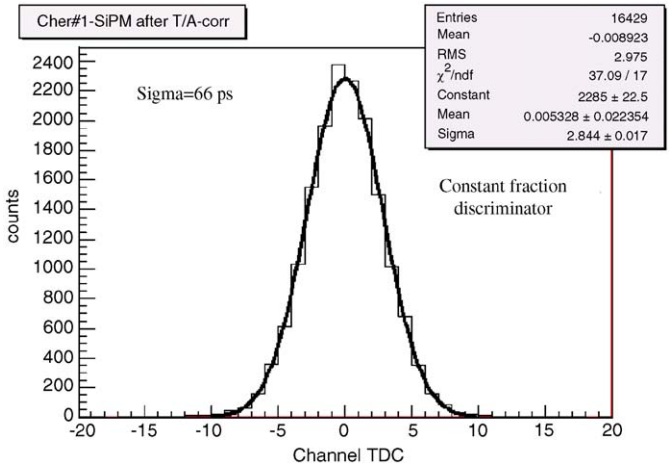

Fig. 8. Timing resolution between: Cherenkov radiator + PMT and BC418 + $3 \times 3\,mm^2$ SiPM for 3 GeV electrons.

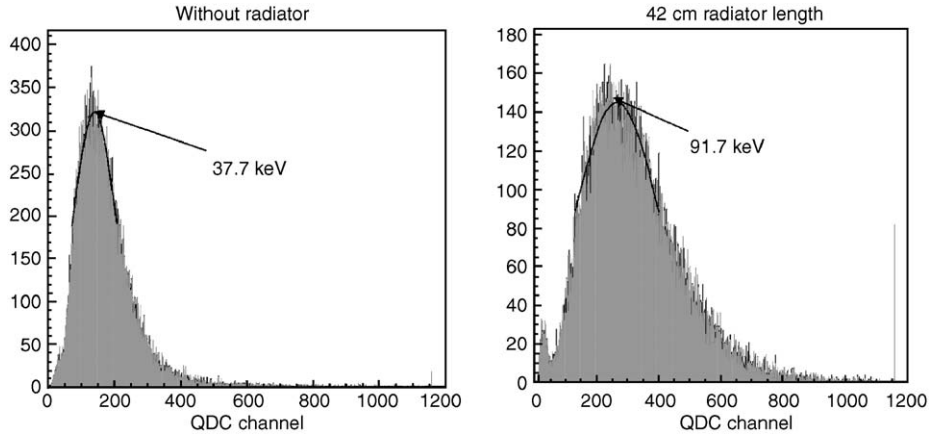

Fig. 7. Pulse height distributions for TR X-ray detection with one polypropylen foils radiator and YAP:Ce crystal + $3 \times 3\,mm^2$ SiPM.

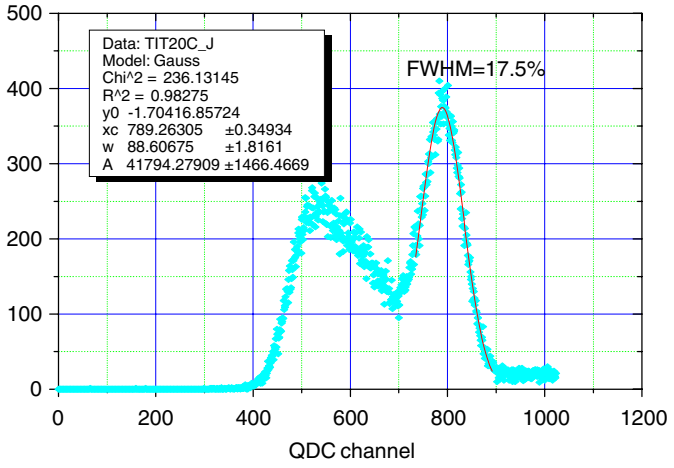

Fig. 9. Pulse height distribution for 511 keV gammas, obtained by LYSO ($3 \times 3 \times 20\,mm^3$) + $3 \times 3\,mm^2$ SiPM system.

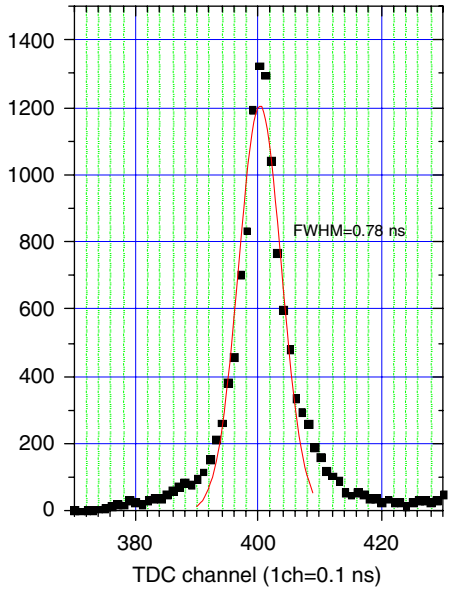

Fig. 10. Timing resolution for two 511 keV gammas obtained by LYSO + $3 \times 3\,mm^2$ SiPM system.

timing in PET by SiPM is demonstrated in Fig. 10, where the time difference between two 511 keV gammas measured with constant fraction discriminators is shown. The timing of 780 ps FWHM has been obtained.

5. Conclusions

New generation of large area SiPM with suppression of OC, AP probability, DR is under development now and will allow to get the SiPMs with:

- area: up to $10 \times 10\,mm^2$;
- PDE: 40–50% in wide wavelength region;
- ENF: 1–1.05;
- subnanosecond timing.

Such step in SiPM developments will increase considerably a number of possible applications of SiPM in the field of particle and astroparticle physics as well as in space and medicine.

Acknowledgements

The authors thanks the CALICE collaboration for help in test beam measurements at DESY. This work is suppoted by ISTC Grant no. 3090-05 and Alexander von Humboldt Foundation Research Award (IV, RUS 1066839 GSA).

References

[1] A. Goetzbergen, B. McDonald, R.H. Haitz, R.M. Scarlett, J. Appl. Phys. 34 (1963) 1591;
R.H. Haitz, J. Appl. Phys. 35 (1965) 3123;
P.P. Webb, R.J. McIntyre, Bull. Am. Phys. Soc., Ser. Ii-15 (1970) 813.
[2] S. Cova, M. Ghioni, A. Lacaita, C. Samori, F. Zappa, Appl. Opt. 35 (1996) 1956.
[3] G. Bondarenko, B. Dolgoshein, V. Golovin, A. Ilyin, R. Klanner, E. Popova, Nucl. Phys. B (Proc. Suppl.) 61B (1998) 347 and reference therein.
[4] Z. Sadygov, talk given at Beaune-2005 and references therein, these proceedings.
[5] S. Cova, M. Ghioni, A. Lotito, I. Rech, F. Zappa, Evolution and prospects of SPAD's and quenching circuits, talk given at NIST Workshop on Single Photon Detectors, USA, 2003.
[6] P. Buzhan, B. Dolgoshein, V. Kanzerov, V. Kaplin, A. Karakash, F. Kayumov, S. Klemin, N. Kondratieva, A. Pleshko, E. Popova, presentation at Beaune-2005, these proceedings.
[7] P. Buzhan, B. Dolgoshein, L. Filatov, A. Ilyin, V. Kanzerov, V. Kaplin, A. Karakash, F. Kayumov, S. Klemin, E. Popova, S. Smirnov, Nucl. Instr. and Meth. A 504 (2003) 48.
[8] A.N. Otte, J. Barral, B. Dolgoshein, J. Nose, S. Klemin, E. Lorenz, R. Mirzoyan, E. Popova, M. Teshima, Nucl. Instr. and Meth. A 545 (2005) 705.